ARTICLE

Alterations in white matter microstructure in individuals at persistent risk for psychosis

David R. Roalf[1] · Angel Garcia de la Garza[1] · Adon Rosen · Monica E. Calkins[1] · Tyler M. Moore[1] · Megan Quarmley[1] · Kosha Ruparel[1] · Cedric Huchuan Xia[1] · Petra E. Rupert[1] · Theodore D. Satterthwaite[1] · Russell T. Shinohara[2] · Mark A. Elliott[3] · Ruben C. Gur[1,3,4] · Raquel E. Gur[1,3,4,5]

Abstract

Abnormalities in brain white matter (WM) are reported in youth at-risk for psychosis. Yet, the neurodevelopmental time course of these abnormalities remains unclear. Thus, longitudinal diffusion-weighted imaging (DWI) was used to investigate WM abnormalities in youth at-risk for psychosis. A subset of individuals from the Philadelphia Neurodevelopmental Cohort (PNC) completed two DWI scans approximately 20 months apart. Youths were identified through structured interview as having subthreshold persistent psychosis risk symptoms ($n = 46$), and were compared to healthy typically developing participants (TD; $n = 98$). Analyses were conducted at voxelwise and regional levels. Nonlinear developmental patterns were examined using penalized splines within a generalized additive model. Compared to TD, youth with persistent psychosis risk symptoms had lower whole-brain WM fractional anisotropy (FA) and higher radial diffusivity (RD). Voxelwise analyses revealed clusters of significant WM abnormalities within the temporal and parietal lobes. Lower FA within the cingulum bundle of hippocampus and cerebrospinal tracts were the most robust deficits in individuals with persistent psychosis symptoms. These findings were consistent over two visits. Thus, it appears that WM abnormalities are present early in youth with persistent psychosis risk symptoms, however, there is little evidence to suggest that these features emerge in late adolescence or early adulthood. Future studies should seek to characterize WM abnormalities in younger individuals and follow individuals as subthreshold psychotic symptoms emerge.

✉ David R. Roalf
roalf@pennmedicine.upenn.edu

1   Brain Behavior Laboratory, Department of Psychiatry, Neuropsychiatry Section, Perelman School of Medicine, University of Pennsylvania, Philadelphia, PA 19104, USA

2   Department of Biostatistics and Epidemiology, Perelman School of Medicine, Philadelphia, PA 19104, USA

3   Department of Radiology, Hospital of the University of Pennsylvania, Philadelphia, PA 19104, USA

4   Lifespan Brain Institute (LiBI) at the University of Pennsylvania and Children's Hospital of Philadelphia, Philadelphia, PA 19104, USA

5   Department of Child and Adolescent Psychiatry, Children's Hospital of Philadelphia, Philadelphia, PA 19104, USA

Introduction

Psychosis is a complex brain disorder that typically emerges in late adolescence or early adulthood [1], enormously impacts functioning, and results in large costs to public health [2]. There are significant brain abnormalities in psychosis, including progressive brain tissue loss [3], reduced neuropil in the cortex [4], altered dopaminergic function [5], abnormal glutamate functioning [6], and alterations in brain white matter (WM) organization [7, 8]. This constellation of dysfunction may exist from birth, which allows for the study of specific biological targets associated with psychosis; many of which may abnormally progress during the course of adolescent neuromaturation [9]. Recent advances in neuroimaging, including the use of diffusion-weighted imaging (DWI), has led to a better understanding of effects of disrupted white matter organization, and has the potential to allow for both earlier identification of illness and targeted treatments.

Early intervention requires valid and reliable methods of identifying youth at highest risk for developing psychosis. Youths with subpsychotic symptoms often exhibit subtle neurobiological abnormalities like those found in psychosis [10, 11]. Hence, many contemporary investigations focus on individuals at clinical high risk (CHR) for developing psychosis, or at-risk mental states, in both help-seeking [12], and community-based samples [13, 14]. When individuals at risk are followed over time about 30% develop a psychotic disorder within 2 years [15], most commonly schizophrenia (SZ) [15]. Many of the deficits in cortical microcircuitry in psychosis are found to some extent in CHR, including disrupted neurotransmission [16], lower gray matter volume [17], and disruptions of white matter microstructure organization [18]. These anomalies may reflect aberrant brain development, and quantification of these features has the potential to enhance our ability to detect those truly at risk for developing psychosis.

DWI has facilitated the in vivo study of brain WM microstructural organization. DWI measures the diffusion of water molecules through brain tissue, a process that is affected by microstructural properties of the local surrounding tissue [19, 20]. Disrupted WM microstructure, as indicated by low-fractional anisotropy (FA) and high diffusivity, is documented in numerous brain regions in chronic SZ [7], while more recent investigations of early-onset psychosis [21] and psychosis in adolescence [22] report focal WM abnormalities. Typically, these findings are limited to major WM fiber tracts including the cingulum bundle (CB), corpus callosum, and anterior limb of the internal capsule [23]. Given recent convergent evidence that psychosis is a product of abnormal neurodevelopment, it is not surprising that WM microstructure is also aberrant in CHR individuals [24, 25].

Yet, longitudinal diffusion imaging studies of brain WM in early psychosis and youths with psychosis spectrum symptoms are scant [26, 27]. In fact, there are only two longitudinal studies in early-onset psychosis [28, 29] and two in youth at clinical high-risk for psychosis [30, 31]. Early-onset psychosis [28] is associated with increasing FA over 2.5 years, which was not found in healthy comparison subjects, suggesting delayed maturation. Another study [29] found early-onset psychosis patients had lower FA in comparison to healthy comparison subjects, but there was no evidence that this difference changed over time. Individuals at risk for developing psychosis [30] show associations between lower FA and negative symptoms, but DWI data from this 1.5 T magnetic resonance imaging (MRI) study was limited to only the corpus callosum. Another study in at-risk youth, found association between increased FA in the superior longitudinal fasciculus and age, again suggesting delayed maturation, although the follow-up interval was only 12 months [31]. Thus, more longitudinal diffusion imaging studies are needed to directly test current models of the development and lifetime course of brain structure associated with psychosis risk.

Here, we measure WM microstructure, longitudinally, in a large community sample of youths with and without subthreshold psychosis risk symptoms. Clinical symptoms and DWI were measured at two time points over approximately 20 months in individuals with persistent psychosis symptoms and typically developing (TD) youths. To our knowledge, there are no previous studies of this size in community youth with persistent symptoms that have been followed over time and where developmental WM abnormalities were measured. Evidence of WM disruption in this sample would provide convergent support for the examination of WM microstructure as a phenotype for individuals on the psychosis spectrum.

Our hypotheses were as follows: (1) age-related increases in FA and age-related decreases in diffusivity; (2) PS individuals with persistent symptoms would show abnormalities (e.g., lower FA; higher diffusivity) in WM microstructure in regions impacted in adults with psychosis; (3) WM abnormalities will progressively worsen with time in PS youth; and (4) alterations in diffusion metrics will be associated with clinical symptoms and cognitive performance.

Methods and materials

All participants included in this study were initially enrolled in the Philadelphia Neurodevelopmental Cohort [13, 14, 32, 33] and provided informed consent or, for minors, informed assent plus parental consent. All procedures were approved by the Institutional Review Boards of the University of Pennsylvania and Children's Hospital of Philadelphia.

Participant recruitment

Briefly, participants were recruited by the Center for Applied Genomics at CHOP through a pediatric healthcare network of over 30 clinical community sites in the tristate area of Pennsylvania, New Jersey, and Delaware. Initial recruitment occurred between 2006 and 2012, which is described in full in a previous report [13]. When undergoing blood work, patients were approached for participation in the recruitment pool. The percentage of patients undergoing blood work across recruitment sites varied from 11 to 53%, with a mean of 36%. Participants provided a blood sample for genomic studies and access to electronic medical records (EMRs). The EMR of each participant was screened for preliminary eligibility for Philadelphia Neurodevelopmental Cohort (PNC) participation. Potential participants were included if they were between the ages of 8–21, had

provided written informed consent/assent to be recontacted for future studies, were proficient in English, and did not appear to have significant developmental delays or physical conditions that would interfere with their ability to complete study procedures. Of the initial recruitment pool, 9498 completed clinical and cognitive assessment. A random subsample ($n = 1601$), stratified by age and gender, were enrolled in neuroimaging [34].

Socioeconomic background was calculated using an environmental factor score [35], which incorporates neighborhood-level features based on geocoding (crime, median family income, etc.; see Supplement). Selected individuals from the imaging subsample were re-contacted for follow-up visits. Individuals who underwent follow-up MRI: (1) completed the MRI protocol during initial enrollment and (2) had either the presence of psychosis spectrum symptoms at the initial visit or were free of any psychopathology and/or medical conditions (e.g., healthy; Fig. 1).

Initial clinical assessment (Time 1)

The initial clinical assessment included three structured screening tools to assess broad spectra of psychosis-relevant experiences and other psychopathology. Descriptions of the assessment tools and threshold classification criteria are published [13, 14]. Briefly, subjects were classified as "Psychosis Spectrum" (PS) if they exceeded the threshold on the psychosis spectrum screen, regardless of the presence or absence of other psychopathology. Subjects were classified as "Other Psychopathology" (OP) if they did not meet criteria for PS, but exceeded criteria for one or more other psychopathology domains. Subjects were classified as "healthy" (HC) if they did not meet criteria for either PS or OP. Subjects were further screened and excluded if they had significant comorbid medical conditions, as previously described [34]. Additional detail is provided in the Supplement.

Follow-up clinical assessment (Time 2)

Mean time to clinical follow-up occurred 20.4 months after the initial visit; the range of follow-up was between 9 and 40 months. Descriptions of the assessment tools and threshold classification criteria at follow-up are published [36, 37]. All participants received comprehensive clinical assessments including a semistructured diagnostic interview to assess a broad spectrum of psychosis-relevant experiences [36]. Individuals were classified as CHR for psychosis if they had at least one positive OR two negative, and/or disorganized symptoms rated 3, 4, or 5 on the Scale of Prodromal Symptoms [38], without meeting criteria for a DSM-IV Axis I psychotic disorder. Six individuals met criteria for a psychotic disorder (PSY) at follow up. Again,

subjects were classified as "Other Psychopathology" (OP) if they did not meet criteria for PS, but met DSM-IV criteria for one or more other psychopathology domains. Healthy individuals (HC) had no DSM-IV Axis I psychotic disorder, no super-threshold prodromal symptomatology, no history of psychosis in a first-degree biological relative, and no personal Axis II Cluster A diagnosis. All individuals received functioning (Global Assessment of Functioning (GAF) [39]) screening inventories.

Longitudinal clinical categorization

To evaluate the stability of WM microstructure as a relevant phenotype in psychosis risk, individuals were classified based upon the combination of the Time 1 and Time 2 clinical labels (Fig. 1). Given our interest in psychosis we focused our analyses on the comparison between those with persistent psychosis risk symptoms and those that were consistently healthy. If an individual was PS at the initial visit and CHR or PSY at follow-up, he/she was considered "Persistent" for psychosis risk. The "Typically Developing" (TD) group comprised healthy individuals who were free of significant psychopathology at both visit one and two. The number of months between clinical visits was similar for persistent psychosis risk [23.51 (6.66)] and TD [22.57 (6.49); $t(96) = 1.20$, $p = 0.23$].

Computerized neurocognitive battery

Cognitive ability was measured using the Penn Computerized Neurocognitive Battery (CNB). [33] We examined global factor scores for cognitive accuracy, speed, and efficiency, which have been examined previously [40] in relation to WM microstructure. In general, the CNB was collected on the same day as the clinical assessment. The number of months between CNB examinations was similar for persistent psychosis risk [23.55 (6.70)] and TD [22.79 (6.38); $t(96) = 1.20$, $p = 0.23$].

Neuroimaging

MRI scans were acquired on the same 3T Siemens Tim Trio whole-body scanner, used the same 32-channel head coil and acquisition protocol. Data were collected between 2009 and 2013. The average duration, in months, between MRI scans was similar for persistent psychosis risk [20.06 (6.25)] and TD [19.18 (6.40); $t(96) = 0.96$, $p = 0.33$]. The range of MRI follow-up was 7–35 months.

Diffusion imaging sample

At Time 1, 38 persisters and 79 TD had usable DWI data, while at Time 2, 37 persisters and 89 TD had usable DWI
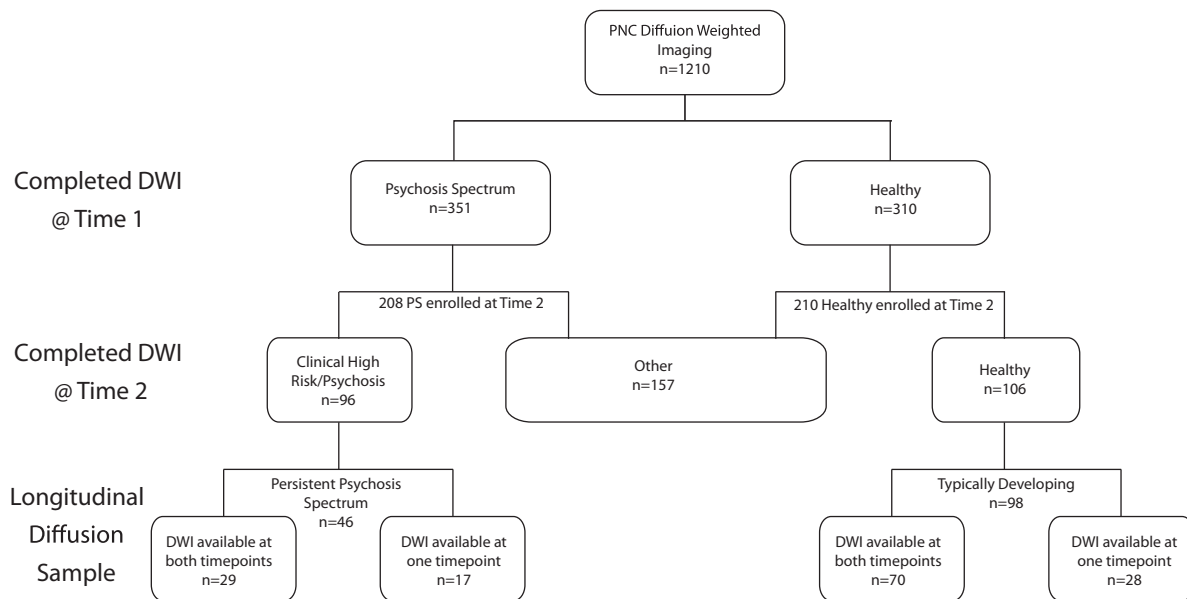
Fig. 1 Flow diagram of persistent psychosis and typically developing youth as enrolled and followed as part of the Philadelphia Neurodevelopmental Cohort. Of the 1601 individuals imaged as part of the PNC, 452 individuals screened positive for psychosis spectrum (PS) symptoms and 498 were considered healthy. At follow-up, 208 PS and 210 healthy were re-enrolled. Of these, 106 PS has persistent or worsening symptoms, while 153 healthy were still considered healthy. Of those imaged at follow-up, 46 youth with persistent psychosis risk symptoms and 98 TD had high-quality diffusion-weighted imaging acquired. Note: Not all individuals at baseline or follow-up completed the DWI portion of the neuroimaging protocol [32, 34] or data quality was considered too poor for analysis [41]

data (Fig. 1). Of these individuals, 29 persisters and 70 TD had complete clinical and DWI data passing QA (see DWI quality control in Supplementary Material) from *both* Time 1 and Time 2. Thus, a mixed-model statistical approach was used to take advantage of all available data. Applying a mixed effects model allowed for the use of all observations without list-wise deletion. Individuals were excluded based on health and medical history, incidental radiologic findings, and for poor DTI image quality, including both manual and automated image quality assessment [41]. At Time 1, ten persisters were taking psychoactive medications, most commonly stimulants (Table 1). At Time 2, those medicated at Time 1 remained medicated and four additional individuals were taking psychoactive medications. A summary table of medications is provided Supplementary Table 4.

DWI acquisition, quality control, and processing

As previously described [32, 41], DWI scans were obtained using a twice-refocused spin-echo single-shot EPI sequence (See Supplement for sequence details). The complete sequence consisted of 64 diffusion-weighted directions with $b = 1000$ s/mm [2] and 7 interspersed scans where $b = 0$ s/mm^2 [32]. A B0 field map was acquired and used in the preprocessing [41]. Images were checked for data quality using manual and automated methods, which are publicly available, [41] (https://davidroalf.com/qascripts).

QC metrics include temporal signal-to-noise (TSNR) and mean relative motion. Following QC, diffusion data were skull stripped by generating a brain mask for each subject by registering a binary mask of a standard image (FMRIB58_FA) to each subject's brain using FLIRT [42]. When necessary, manual adjustments were made to this mask. Next, eddy currents and head motion were estimated and corrected using FSL's eddy tool [41, 43, 44]. The diffusion gradient vectors were rotated to adjust for motion using eddy's six-parameter motion output. The field map was estimated and distortion correction was applied to the DWI data using FSL's FUGUE [42]. Finally, the diffusion tensor was modeled and metrics were estimated at each voxel using FSL's DTIFIT.

Registration from native space to a template space was completed using DTI-TK [45]. First, the DTI outputs of DTIFIT were converted to DTI-TK format and registered to PNC-specific template; the details of this procedure are published [41]. All DTI maps were then registered (rigid, affine, and diffeomorphic) to the high-resolution study-specific template using DTI-TK. FA, MD, AD, and RD were compared along a study-specific WM skeleton. Mean diffusion metrics were extracted from ten full regions of interest (ROI; ICBM-JHU White Matter Tracts; Harvard-Oxford Atlas; Supplementary Table 1) using FSL's "fslmeans" command and averaged across ROI. Additional details are provided in the Supplement.

Table 1 A comparison of participant demographic, clinical and cognitive scores by diagnostic group

	Persistent psychosis risk Initial	Persistent psychosis risk Follow-up	Typically developing Initial	Typically developing Follow-up	Statistical analysis[a] Age	Group	Age* group
n	38	37	79	89			
Initial age [range]	15.51 (2.52) [11.50–21.41]	16.82 (2.61) [12.75–22.50]	16.64 (2.82) [11.33–21.75]	17.38 (3.56) [11.25–23.58]	**$F_{(1,97)} = 741.09, p < 0.001$**	$F_{(1,168)} = 1.17, p = 0.28$	$F_{(1,97)} = 0.46, p = 0.50$
Sex (% female)	52.60%	40.50%	51.90%	52.80%	**$F_{(1,239)} = 7.22, p = 0.007$**	$F_{(1,239)} = 0.23, p = 0.63$	$F_{(1,239)} = 0.20, p = 0.65$
Race (% Caucasian)	18.40%	27.00%	67.10%	66.30%	$F_{(1,239)} = 0.41, p = 0.52$	**$F_{(1,239)} = 47.90, p < 0.001$**	$F_{(1,239)} = 3.53, p = 0.06$
Handedness (% right)	81.60%	81.10%	83.50%	83.10%	$F_{(1,239)} = 0.42, p = 0.52$	$F_{(1,239)} = 0.08, p = 0.76$	$F_{(1,239)} = 0.60, p = 0.44$
Maternal education[b]	13.79 (2.12)	14.03 (2.62)	15.05 (2.62)	13.55 (4.90)	$F_{(1,185)} = 0.11, p = 0.74$	$F_{(1,130)} = 0.27, p = 0.61$	$F_{(1,185)} = 0.67, p = 0.41$
Paternal education[b]	13.43 (2.52)	12.08 (5.46)	14.74 (2.92)	12.67 (5.76)	$F_{(1,185)} = 1.25, p = 0.27$	$F_{(1,122)} = 0.81, p = 0.37$	$F_{(1,185)} = 0.07, p = 0.79$
Positive symptom score[c]	20.38 (13.47)	12.34 (11.55)	2.01 (4.09)	1.44 (2.88)	**$F_{(1,192)} = 16.50, p < 0.001$**	**$F_{(1,137)} = 125.83, p < 0.001$**	**$F_{(1,192)} = 10.78, p = 0.001$**
Negative symptom score[d]	0.96 (0.76)	1.14 (0.74)	0.09 (0.17)	0.09 (0.24)	$F_{(1,194)} = 1.49, p = 0.22$	**$F_{(1,148)} = 180.54, p < 0.001$**	$F_{(1,194)} = 2.04, p = 0.15$
Global function score (z score)[e]	−1.77 (1.68)	−1.98 (1.03)	0.24 (0.86)	0.24 (0.97)	$F_{(1,164)} = 0.54, p = 0.16$	**$F_{(1,118)} = 148.51, p < 0.001$**	$F_{(1,164)} = 3.06, p = 0.08$
TSNR[f]	7.31 (0.38)	7.15 (0.26)	7.43 (0.39)	7.28 (0.38)	**$F_{(1,184)} = 22.98, p < 0.001$**	**$F_{(1,36)} = 7.64, p = 0.006$**	$F_{(1,184)} = 1.34, p = 0.25$
Average head motion[g]	0.42 (0.27)	0.41 (0.26)	0.33 (0.16)	0.34 (0.18)	$F_{(1,185)} = 0.24, p = 0.90$	**$F_{(1,143)} = 5.14, p = 0.02$**	$F_{(1,185)} = 0.07, p = 0.78$
Psychoactive Medications[h]	10	14	0	0	$F_{(1,122)} = 0.02, p = 0.90$	**$F_{(1,122)} = 23.88, p < 0.001$**	$F_{(1,122)} = 0.28, p = 0.60$
CNB accuracy[i]	−0.27 (1.07)	−0.08 (1.17)	0.48 (0.78)	0.50 (0.75)	**$F_{(1,233)} = 33.95, p < 0.001$**	**$F_{(1,138)} = 19.09, p < 0.001$**	$F_{(1,233)} = 0.54, p = 0.48$
CNB speed[h]	−0.30 (1.26)	0.11 (0.99)	0.19 (0.86)	0.45 (0.82)	$F_{(1,206)} = 1.28, p = 0.08$	**$F_{(1,140)} = 6.45, p = 0.01$**	$F_{(1,206)} = 0.58, p = 0.45$
CNB efficiency[i]	−0.40 (1.14)	−0.02 (1.07)	0.42 (0.82)	0.64 (0.69)	**$F_{(1,226)} = 23.18, p < 0.001$**	**$F_{(1,133)} = 19.95, p < 0.001$**	$F_{(1,233)} = 0.32, p = 0.86$
Environment score[j]	−0.57 (1.01)	−0.40 (1.07)	0.16 (0.95)	0.20 (0.93)	$F_{(1,239)} = 0.17, p = 0.68$	**$F_{(1,239)} = 25.79, p < 0.001$**	**$F_{(1,239)} = 13.07, p = 0.003$**

[a]Mixed effects modeling was used to compare demographic variables by age and diagnostic group. Otherwise, ANOVAs (e.g., sex, rage, handedness, and environment score) were used to compare demographic variables by age and diagnostic group where appropriate. Significant differences are highlighted in bold text

Note: For age, visit number was used as the independent measure. Age was centered for all analyses.

Values are shown as mean ± standard deviations

[b]Values are shown in years

[c]SIPS-positive items [14]

[d]SIPS-negative items [14]

[e]Global assessment of functioning scale

[f]Temporal signal-to-noise ratio [41]

[g]Mean relative root mean squared motion [41]

[h]See Supplementary Table 4

[i]CNB factor scores [35]

[j]Environment score [35]

Statistical analysis

Demographic, clinical and cognitive group differences were examined with chi-square, *t* tests and analysis of covariances, where appropriate. Prior work has demonstrated that brain development [46], including WM development [47], is not a linear process. Thus, group-level analyses of DTI data were flexibly modeled using penalized splines within a mixed effects generalized additive mixed model (GAMM [48, 49]). The GAMM is a commonly used statistical approach [50, 51] that assesses a penalty for increasing nonlinearity to avoid over-fitting and allows for structured errors such as those observed in longitudinal studies.

The following GAMM model used was:

$$DWI\,scalar\,metric\,(FA/MD/RD/AD)$$
$$\sim s(AgeAtScan, k = 4) + diagnosis + sex + race$$
$$+ DWITSNR, random\,factor = 1|subject.$$

Diffusion (FA, MD, AD, and RD), clinical and cognitive measures were modeled as the dependent measure, while the spline of age and diagnostic group were modeled as independent factors. Interaction terms (diagnosis*age) were tested, but not significant (See Supplementary material), thus these were not included in the final model. All models were controlled for potentially confounding effects of sex, race, and TSNR. Age was mean-centered in all analyses so that the intercept of the model can be interpreted within the age range of the study (See Supplement for additional detail). A *k*-value (smoothness term) of 4 was chosen based upon previous work using GAMM analyses within the PNC data in other brain phenotypes (e.g., ASL and brain structure) [50, 51]. This previous work has found that this *k*-value of 4 tends not to overfit data while allowing enough flexibility over the limited age range of the PNC. The GAMM was implemented in "mgcv" R package [49].

Whole-brain analysis was performed using a customized nonlinear implementation (R-package "voxel") [52] of FSL's randomize [53] to compute tract-based spatial statistics (TBSS) [54], and corrected for multiple comparisons using threshold-free cluster estimation ($p < 0.05$). The GAMM approach was employed for ROI data. False-discovery rate (FDR) was applied to regional data to control for Type-I error probability (*q* value = 0.05); all regional *p* values shown are FDR corrected. Intraclass correlation coefficients (ICCs) were used to measure similarity between scalar brain images and ROIs by scan visit. The I2C2 package in R [55] was used to estimate ICCs for whole-brain images. All statistics were performed using R (3.2.2) statistical software [56].

Results

Participant characteristics and clinical scales

Participant characteristics are shown in Table 1. The diagnostic groups differed in positive and negative symptom scores, GAF, and environment score. Approximately, 30% of youth with persistent symptoms were medicated, most commonly with a stimulant. Positive-symptom scores were significantly lower at Time 2 than Time 1 in psychosis risk youth, but were unchanged in TD. Environment scores, which were only estimated based on Time 1 data, were significantly lower in the persistent youth that returned, while this score was unchanged in those TD who were followed at Time 2.

Computerized neurocognitive battery

Persisters were less accurate, slower and less efficient than TD. This pattern was consistent across time as there was no interaction with age.

DWI data quality

Persisters showed lower TSNR and higher head motion than TD, but there was no interaction with age.

PS youth have disrupted WM microstructure

Nonlinear whole-brain TBSS revealed group differences between persisters and TD in clusters along the major WM skeleton for FA and RD, but not AD or MD (Supplementary Fig. 1). FA differences were found in clusters comprising the forceps major, inferior frontal occipital fasciculus (IFO), CB of the hippocampus (CGH), corticospinal tracts (CST), inferior longitudinal fasciculus (ILF), SLF, and ATR. Differences in RD were limited to a cluster comprising the IFO and Forceps Major. There were no interactions with time. To fully elucidate these limited skeletonized results, diffusion metrics from each JHU White Matter Tract ROI were extracted and analyzed.

Regional analysis

Mean DWI scalars are displayed in Table 2 and complete results of the GAMM analyses are shown in Table 3. Increasing age was associated with higher FA and lower diffusivity values (Supplementary Results).

Lower FA in youth at persistent risk for psychosis

Persisters had lower average WM FA as compared to TD (Fig. 2a). Regional FA (Fig. 3) was lower within the CST,

Table 2 Regional diffusion scalar metrics for typically developing youth and those with persistent pscyhosis symptoms

ROI	TD	Persistent psychosis risk	TD	Persistent psychosis risk	TD	Persistent psychosis risk	TD	Persistent psychosis risk
	Raw FA values		Raw MD values		Raw AD values		Raw RD values	
ATR	0.372	0.366	2.200	2.209	1.038	1.035	0.581	0.587
T1	0.371	0.366	2.203	2.225	1.039	1.043	0.582	0.591
T2	0.373	0.367	2.197	2.193	1.037	1.028	0.580	0.582
CST	0.553	0.548	1.981	1.978	1.121	1.114	0.430	0.432
T1	0.552	0.547	1.987	1.993	1.123	1.122	0.432	0.436
T2	0.555	0.549	1.975	1.963	1.119	1.106	0.428	0.429
CGC	0.536	0.531	2.080	2.071	1.165	1.154	0.458	0.459
T1	0.532	0.530	2.091	2.086	1.167	1.161	0.462	0.462
T2	0.539	0.532	2.070	2.057	1.162	1.146	0.454	0.455
CGH	0.390	0.375	2.146	2.151	1.039	1.027	0.553	0.562
T1	0.388	0.372	2.152	2.173	1.041	1.034	0.555	0.569
T2	0.391	0.379	2.139	2.130	1.036	1.019	0.552	0.555
IFO	0.444	0.437	2.223	2.226	1.137	1.130	0.543	0.548
T1	0.443	0.436	2.228	2.243	1.139	1.138	0.545	0.553
T2	0.445	0.438	2.217	2.209	1.135	1.122	0.541	0.543
ILF	0.471	0.464	2.160	2.171	1.121	1.119	0.519	0.526
T1	0.470	0.462	2.165	2.189	1.123	1.127	0.521	0.531
T2	0.471	0.466	2.156	2.152	1.119	1.112	0.518	0.520
SLF	0.378	0.373	2.170	2.176	1.016	1.014	0.577	0.581
T1	0.376	0.371	2.179	2.193	1.019	1.020	0.580	0.586
T2	0.379	0.375	2.162	2.159	1.013	1.007	0.575	0.576
UF	0.424	0.415	2.183	2.191	1.156	1.145	0.567	0.573
T1	0.422	0.414	2.189	2.207	1.158	1.151	0.570	0.577
T2	0.426	0.416	2.178	2.175	1.154	1.140	0.565	0.569
Forceps major	0.589	0.578	2.291	2.292	1.398	1.420	0.501	0.533
T1	0.590	0.577	2.299	2.305	1.397	1.421	0.496	0.532
T2	0.588	0.579	2.283	2.278	1.400	1.420	0.505	0.534
Forceps minor	0.437	0.434	2.402	2.487	1.208	1.208	0.592	0.597
T1	0.437	0.431	2.394	2.486	1.208	1.214	0.591	0.603
T2	0.438	0.437	2.410	2.488	1.209	1.202	0.593	0.592
Mean whole brain	0.454	0.446	2.393	2.402	1.122	1.117	0.531	0.537
T1	0.452	0.445	2.391	2.420	1.124	1.124	0.532	0.542
T2	0.455	0.448	2.395	2.385	1.120	1.110	0.529	0.532

ATR anterior thalamic radiation, *CST* corticospinal tracts, *CGC* cingulum bundle of the cingulate gyrus, *CGH* cingulum bundle of the hippocampus, *IFO* inferior frontal occipital fasciculus, *ILF* inferior longitudinal fasciculus, *SLF* superior longitudinal fasciculus, *UF* uncinate fasciculus, *TD* typically developing, *T1* Time 1 visit (PNC), *T2* Time 2 visit (follow up)

and the CGH as compared to TD. The intercept of each of these models was significant (*p*s < 0.001; Supplementary Table 6), but there were no interactions with age.

Higher RD in youth at persistent risk for psychosis

Persisters had higher average WM RD ($p_{FDR} < 0.02$) as compared to TD (Fig. 2d). The intercept of this models was significant ($p < 0.001$), but there was no interaction with age. No individual regions differed between persisters and TD. There were no global or regional group differences in MD (Fig. 2b) or AD (Fig. 2c). Results for MD, AD, and age and sex comparisons are presented in the Supplementary Results.

Sensitivity analysis of potential medication effects

Comparisons of demographic and DWI metrics for persistent youth receiving psychoactive medications and those who were not are presented in the Supplementary Tables 3 and 4. All differences between TD and persisters remained significant (except the CST FA) after the exclusion of medicated individuals, but the FDR corrected significance values were smaller.

Similarity of diffusion metrics over time

I2C2 values for diffusion metrics using the TBSS brain mask were: FA = 0.71, MD = 0.57, AD = 0.64, and RD = 0.63.

Table 3 Results of GAMM analyses

ROI	Diagnosis				Sex				Age		EDFs and R^2	
	Beta	Std err	*t*	*p*	Beta	Std err	*t*	*p*	*F*	*p*	*edf	R^2
FA												
ATR	0.0047	0.0027	1.73	1.65E−01	−0.0063	0.0024	*−2.64*	*4.39E−02*	**30.47**	**2.46E−11**	1.93	0.22
CST	0.0109	0.0034	*3.21*	*1.53E−02*	−0.0032	0.0030	−1.08	3.51E−01	**6.75**	**1.71E−03**	1.78	0.09
CGC	0.0087	0.0068	1.28	2.02E−01	−0.0139	0.0060	−2.30	7.41E−02	**32.61**	**2.10E−10**	1.64	0.12
CGH	0.0141	0.0052	*2.72*	*3.53E−02*	−0.0075	0.0046	−1.63	1.72E−01	**6.24**	**2.46E−03**	2.27	0.12
IFO	0.0066	0.0029	2.31	7.34E−02	−0.0015	0.0025	−0.58	6.27E−01	**17.95**	**7.57E−07**	1.74	0.12
ILF	0.0060	0.0038	1.58	1.65E−01	−0.0039	0.0034	−1.17	3.45E−01	**9.50**	**4.07E−04**	1.69	0.07
SLF	0.0051	0.0032	1.58	1.65E−01	−0.0054	0.0028	−1.91	1.14E−01	**17.36**	**2.48E−07**	2.08	0.15
UF	0.0057	0.0039	1.44	1.90E−01	−0.0072	0.0035	−2.07	9.89E−02	**11.94**	**9.27E−04**	1.00	0.09
Forceps major	0.0095	0.0054	1.76	1.65E−01	0.0022	0.0047	0.47	6.38E−01	3.40	6.63E−02	1.00	−0.01
Forceps minor	0.0039	0.0030	1.32	2.02E−01	−0.0119	0.0026	*−4.59*	*7.37E−05*	**14.44**	**1.74E−06**	2.13	0.12
Mean WM	0.0079	0.0026	*3.01*	*2.94E−03*	−0.0060	0.0023	*−2.59*	*1.02E−02*	**25.08**	**2.75E−11**	2.32	0.18
MD												
ATR	0.0262	0.0114	−0.96	4.81E−01	−0.0145	0.0122	2.30	5.52E−02	**16.92**	**3.60E−07**	1.94	0.09
CST	0.0129	0.0089	−1.03	4.81E−01	−0.0212	0.0095	1.45	2.00E−01	**15.73**	**1.29E−06**	1.87	0.16
CGC	0.0385	0.0119	−0.02	9.81E−01	−0.0245	0.0128	*3.25*	*6.32E−03*	**41.36**	**3.08E−09**	1.00	0.17
CGH	0.0157	0.0117	−1.13	4.81E−01	−0.0223	0.0126	1.34	2.00E−01	**26.79**	**1.80E−11**	2.50	0.25
IFO	0.0148	0.0100	−0.80	5.31E−01	−0.0127	0.0108	1.48	2.00E−01	**18.54**	**5.22E−08**	2.23	0.08
ILF	0.0121	0.0123	−1.39	4.81E−01	−0.0097	0.0132	0.99	3.26E−01	**13.83**	**1.79E−06**	2.42	0.09
SLF	0.0191	0.0113	−1.11	4.81E−01	−0.0063	0.0121	1.69	1.84E−01	**9.86**	**6.79E−05**	2.31	0.06
UF	0.0348	0.0111	−1.14	4.81E−01	−0.0229	0.0119	*3.14*	*6.32E−03*	**20.93**	**1.08E−05**	1.00	0.14
Forceps major	−0.0715	0.0514	−1.36	4.81E−01	−0.0677	0.0557	−1.39	2.00E−01	**6.49**	**1.15E−02**	1.00	−0.02
Forceps minor	0.0539	0.0147	−0.65	5.71E−01	−0.0106	0.0159	*3.66*	*3.16E−03*	**4.96**	**6.03E−03**	1.90	0.05
Mean white matter	0.0180	0.0091	−1.68	9.46E−02	−0.0195	0.0098	**1.97**	**4.99E−02**	**19.57**	**2.78E−09**	2.46	0.13
AD												
ATR	0.0068	0.0044	−0.32	9.46E−01	−0.0078	0.0048	1.54	2.50E−01	**13.04**	**7.44E−04**	1.00	0.01
CST	0.0051	0.0048	1.13	7.92E−01	−0.0018	0.0052	1.07	4.10E−01	**18.73**	**1.03E−04**	1.00	0.10
CGC	0.0090	0.0068	1.26	7.92E−01	0.0024	0.0073	1.33	3.07E−01	3.25	7.28E−02	1.00	0.00
CGH	0.0000	0.0054	1.24	7.92E−01	−0.0156	0.0058	−0.01	9.96E−01	**22.78**	**7.73E−09**	2.01	0.23
IFO	0.0061	0.0038	0.85	7.92E−01	−0.0064	0.0041	1.62	2.50E−01	**10.56**	**1.03E−04**	1.99	0.05
ILF	0.0008	0.0048	−0.32	9.46E−01	−0.0085	0.0052	0.17	9.59E−01	**7.58**	**1.33E−03**	1.75	0.04
SLF	0.0030	0.0039	−0.27	9.46E−01	−0.0057	0.0042	0.77	5.52E−01	**5.22**	**2.90E−02**	1.00	−0.01
UF	0.0105	0.0047	−0.07	9.46E−01	−0.0171	0.0051	2.21	1.43E−01	**13.49**	**7.38E−04**	1.00	0.13
Forceps major	−0.0311	0.0186	−0.98	7.92E−01	−0.0230	0.0201	−1.68	2.50E−01	**5.64**	**2.61E−02**	1.00	−0.02
Forceps minor	0.0115	0.0052	−0.08	9.46E−01	−0.0045	0.0056	2.20	1.43E−01	4.01	5.15E−02	1.00	0.00
Mean white matter	0.0031	0.0035	0.31	7.54E−01	−0.0078	0.0038	0.88	3.81E−01	**12.99**	**8.63E−05**	1.33	0.07
RD												
ATR	0.0097	0.0039	−1.22	2.82E−01	−0.0034	0.0042	**2.50**	**3.26E−02**	**21.46**	**5.04E−09**	2.15	0.14
CST	0.0041	0.0032	−2.25	1.26E−01	−0.0101	0.0035	1.28	2.26E−01	**14.77**	**1.12E−06**	2.06	0.14
CGC	0.0159	0.0053	−0.90	3.78E−01	−0.0150	0.0057	**2.98**	**1.22E−02**	**32.97**	**2.38E−10**	1.67	0.19
CGH	0.0080	0.0046	−2.30	1.26E−01	−0.0043	0.0049	1.76	1.33E−01	**20.92**	**1.88E−09**	2.59	0.20
IFO	0.0045	0.0036	−1.53	2.39E−01	−0.0033	0.0039	1.24	2.26E−01	**20.50**	**6.20E−09**	2.25	0.10
ILF	0.0059	0.0045	−1.67	2.39E−01	−0.0005	0.0048	1.31	2.26E−01	**14.82**	**6.45E−07**	2.48	0.11
SLF	0.0085	0.0042	−1.39	2.39E−01	−0.0007	0.0045	2.03	8.61E−02	**13.98**	**1.12E−06**	2.45	0.11
UF	0.0125	0.0042	−1.42	2.39E−01	−0.0030	0.0046	**2.94**	**1.22E−02**	**18.59**	**2.95E−05**	1.00	0.12
Forceps major	−0.0204	0.0168	−1.54	2.39E−01	−0.0220	0.0182	−1.22	2.26E−01	**5.27**	**2.26E−02**	1.00	0.00
Forceps minor	0.0212	0.0051	−0.88	3.78E−01	−0.0030	0.0055	**4.14**	**4.86E−04**	**7.46**	**7.72E−04**	2.13	0.08
Mean white matter	0.0076	0.0032	*−2.47*	*1.42E−02*	−0.0060	0.0035	**2.34**	**2.01E−02**	**23.73**	**2.51E−11**	2.58	0.17

ATR anterior thalamic radiation, *CST* corticospinal tracts, *CGC* cingulum bundle of the cingulate gyrus, *CGH* cingulum bundle of the hippocampus, *IFO* inferior frontal occipital fasciculus, *ILF* inferior longitudinal fasciculus, *SLF* superior longitudinal fasciculus, *UF* uncinate fasciculus, *TD* typically developing, *edf* estimated degrees of freedom. Significant differences are highlighted in bold text

ICCs are shown for each diagnostic group in Table 4 for DWI scalars. ICCs for each ROI and each whole brain measure were significant ($ps < 2.08 \times 10^{-5}$) and ranged from 0.44 for MD in the CB in to 0.97 for MD in the forceps major. In general, FA values had higher ICCs than measures of diffusivity.

Table 4 Intraclass correlation coefficients by region in typically developing youth and those with persistent psychosis risk symptoms

ICCs	Typically developing				Persistent psychosis risk			
	FA	MD	AD	RD	FA	MD	AD	RD
ATR	0.65	0.67	0.70	0.68	0.71	0.61	0.72	0.62
CST	0.77	0.59	0.71	0.66	0.86	0.77	0.81	0.81
CGC	0.84	0.44	0.70	0.65	0.82	0.62	0.75	0.71
CGH	0.72	0.47	0.57	0.52	0.79	0.56	0.69	0.65
IFO	0.82	0.73	0.71	0.77	0.74	0.63	0.65	0.66
ILF	0.83	0.72	0.70	0.78	0.78	0.71	0.74	0.74
SLF	0.70	0.50	0.53	0.57	0.85	0.62	0.55	0.70
UF	0.81	0.62	0.70	0.69	0.76	0.66	0.76	0.68
Forceps major	0.89	0.97	0.96	0.96	0.90	0.97	0.97	0.97
Forceps minor	0.85	0.81	0.77	0.85	0.87	0.79	0.69	0.84
Mean	0.78	0.67	0.62	0.71	0.81	0.71	0.71	0.74

Associations with clinical symptoms and neurocognitive performance

Higher average MD ($p = 0.004$), AD ($p = 0.03$), and RD (0.003) was associated with higher positive symptom scores across TD and persisters. The same relationship was observed for the ILF (MD ($p = 0.005$), AD ($p = 0.03$), RD ($p = 0.003$)) and the IFO (MD ($p = 0.005$), RD ($p = 0.003$)). When analysis included only persisters, this relationship was restricted to mean AD ($p = 0.03$) and MD ($p = 0.04$); see Supplementary Fig. 2A, B. There were no associations with negative symptoms or GAF.

Higher average MD ($p = 0.04$) and mean AD ($p = 0.04$) were associated with lower CNB efficiency factor scores across TD and persisters (Supplementary Fig. 2C,D). Regionally, higher AD within the CST and UF, and higher RD within the CGH were associated with lower CNB efficiency factor scores. There were no interactions between diagnosis and clinical or cognitive performance for any diffusion outcome measure.

Discussion

Using targeted longitudinal follow-up of a large community-based sample, we identified abnormalities of WM microstructure in youth with persistent psychosis risk symptoms. As expected, non-linear age-related changes in DTI scalar measures were present in both persisters and TD. Lower average and regional whole-brain FA and higher RD were present in individuals with risk symptoms that were followed longitudinally over approximately 2 years. Lower FA was maximal within the cerebrospinal tracts and the CB of the hippocampus. Yet, there was no interaction between

age and diagnosis on DTI scalar measures. Higher whole-brain MD and AD were both associated with higher positive symptoms in individuals with persistent psychosis risk and lower cognitive efficiency across all participants. Overall, these findings delineate a pattern of localized, abnormal microstructural brain development in youth with persistent subthreshold psychosis symptoms.

Longitudinal studies of WM changes in psychosis and psychosis risk are rather limited and previous results vary. Our results are similar to one previous study in early-onset SZ-spectrum disorders, in that we find altered diffusion in brain WM (e.g., lower FA), without progressive worsening of these WM abnormalities. Yet, our findings differ from that of the only previous longitudinal study in CHR youth [30]. We did not find lower FA in the corpus callosum (e.g., forceps major/forceps minor), nor an association with negative symptoms. In fact, our findings indicate an association with positive symptoms. Methodological differences between these studies are important to consider as in Saito et al. [30] the follow-up time was shorter (12 months), FA was only measured in the callosum, and the study was completed at 1.5 T with limited data quality assurance. Yet, the overall conversion rate to clinical psychosis was similar in each study (13% in the present study and 15% in Saito et al.). Our findings in youth with persistent psychosis-like symptoms add to a growing literature of WM disruptions in youth at risk for psychosis, but importantly, indicate that this dysfunction is present in a sample of individuals with persistent *subthreshold* clinical symptoms.

The specific reduction in FA within the lateral temporal aspect of the CB (e.g., CGH) is intriguing given the significant connections that this WM tract has with key brain structures known to affect symptoms and cognition in psychosis [57]. The CB is a prominent WM tract comprising long and short-range fibers that support interactions among the prefrontal, parietal, and temporal lobes [58–60]. The CB has connections with regions associated with memory and executive functioning including the thalamus, amygdala, hippocampus, and dorsolateral and dorsomedial prefrontal cortex [61]. Importantly, recent neuroanatomical evidence indicates distinct subdivisions of the cingulum—including a lateral temporal subdivision with specific connections between the parahippocampus and the frontal and parietal lobes [62]. This aspect of the CB is a "control" pathway supporting memory, executive function and other cognitive functions [63]. It is within this specific subdivision of the cingulum that we find significantly lower FA in youth with persistent psychosis-like symptoms. Thus, it is possible that brain regions associated with this aspect of the cingulum are the earliest to exhibit neuronal dysfunction in this sample and may contribute to higher positive symptoms and/or lower cognitive efficiency reported in the current study. Indeed, a recent study using a cross-sectional sample

Fig. 2 Mean (±95% CI) whole brain diffusion metrics in typically developing (TD) and persistent psychosis risk. On average, those with persistent psychosis risk had lower average fractional anisotropy and higher radial diffusivity as compared to TD. Fitted values across the two time points are shown for each individual in the left panel for each metric. There were no group differences in mean or axial diffusivity. Analyses were corrected for linear and non-linear effects of age, and sex, race, and temporal signal-to-noise ratio. Age was centered for all analyses. $*p < 0.05$, FDR corrected
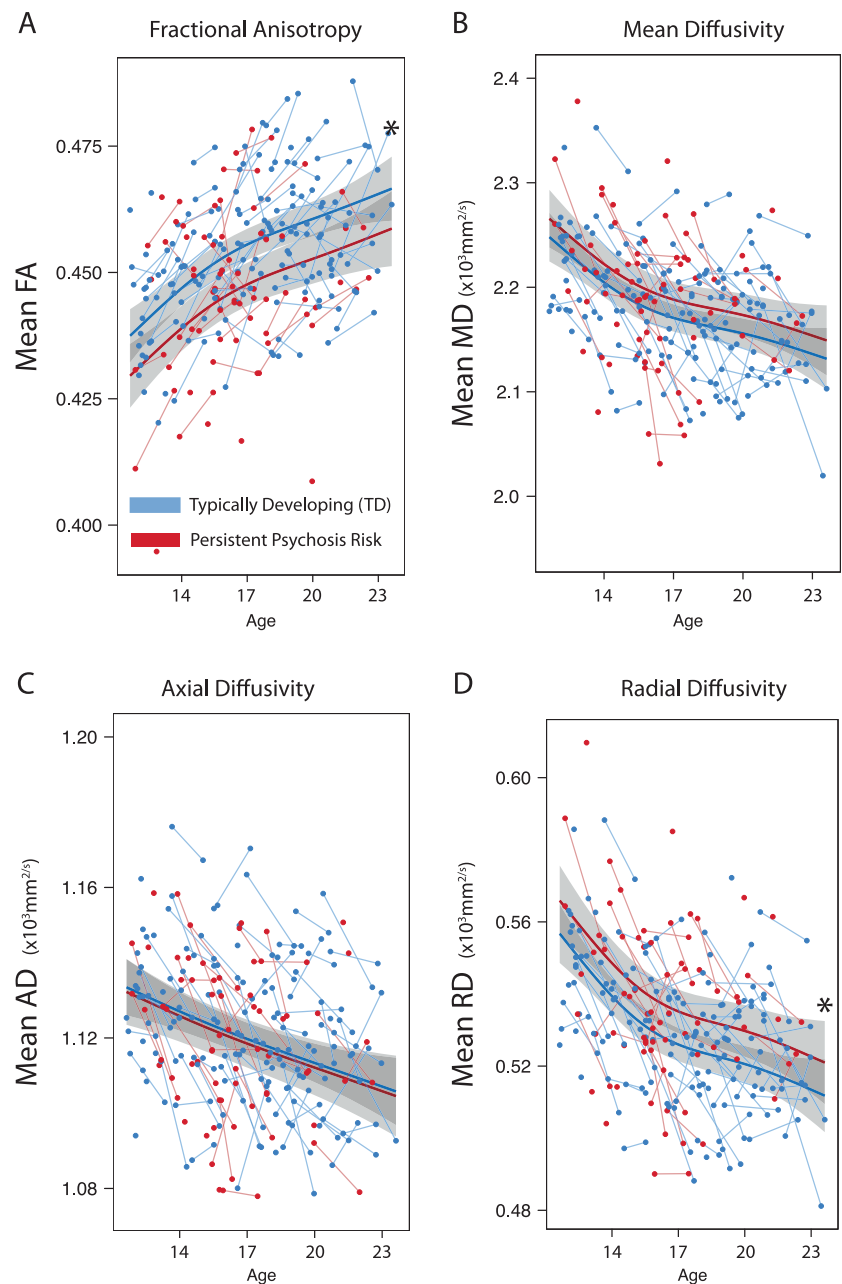
of psychosis spectrum youth from the PNC found these individuals to have lower gray matter volume within the medial temporal lobe [50], which was associated with higher positive symptoms. Yet, we acknowledge that most associations between diffusion measures and symptoms and cognitions were limited to average whole brain measures. As such, the specificity of these associations remains to be elucidated.

It is tempting to compare the similarity of our findings to those in help-seeking samples and to patients with documented psychosis. For example, altered WM organization, as indicated by lower FA and high diffusivity, is well documented in numerous brain regions in chronic SZ [7, 8],

early-onset psychosis [21], psychosis in adolescence [22], and youth at risk for developing psychosis [18]. Typically, these findings are seen in major WM fiber tracts including the corpus callosum, anterior limb of the internal capsule, and CB [23]. However, we must consider that young adults can present with highly variable clinical symptoms during the psychosis risk period and that many will not develop significant psychotic disorders. Moreover, these individuals may also exhibit depression, anxiety, attention deficit, and conduct disorder symptoms [13, 36]. Yet, brain WM measures may be useful even when the psychosis risk diagnosis is unambiguous. Ultimately, assessing the predictive utility of these measures requires studies that track brain
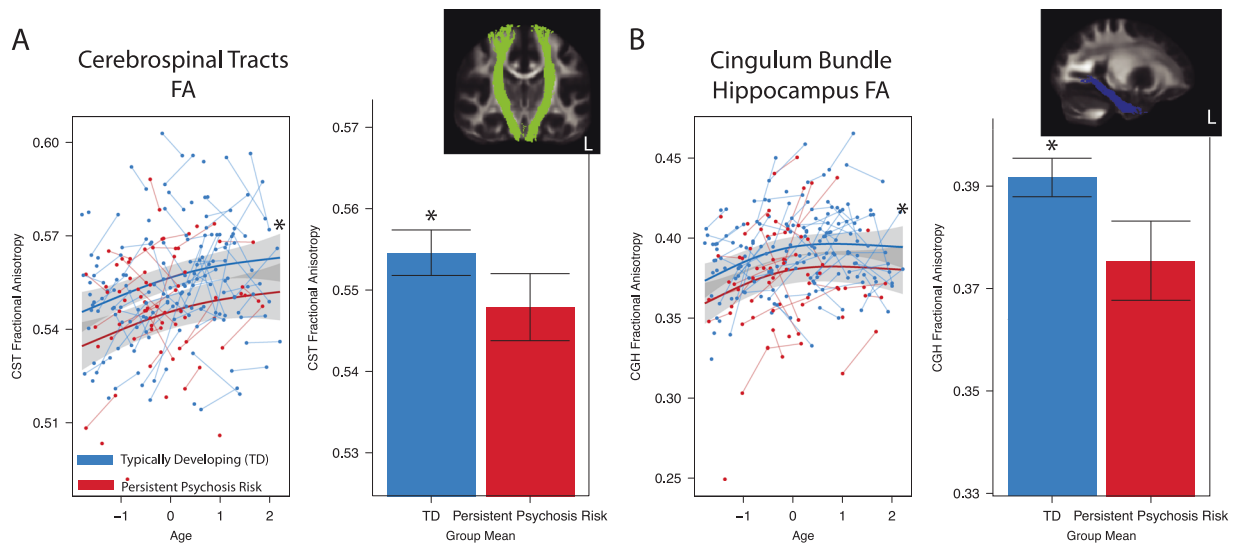
Fig. 3 Regional differences in fractional anisotropy (FA) in typically developing (TD) and persistent psychosis risk. On average, those with persistent psychosis risk had lower average fractional anisotropy in the cerebrospinal tracts (CST) and the cingulum bundle of the hippocampus (CGH) as compared to TD. There were no group differences in regional MD, RD, or AD. Analyses were corrected for linear and non-linear effects of age, and sex, race, and temporal signal-to-noise ratio. Age was centered for all analyses. *$p < 0.05$, false discovery rate (FDR) corrected. Mean (±95% CI)

development earlier in youth and follow individuals over the long-term to determine final clinical outcomes. Nonetheless, we note the consistent parallels between what we observe here in the prepsychotic-risk period and the findings reported in psychosis patients. Identifying these common neurobiological markers prior to the emergence of super-threshold symptomatology may enhance prediction and facilitate earlier intervention.

In order to assess whether WM abnormalities were already present or emerged during the time frame of the current study we investigated the intercept for those measures with significant group effects. The intercept was highly significant suggesting that the diffusion values (FA and RD) at the mean age of our sample differ and are consistently different across all ages included in the current study (e.g., no interaction with age). For example, mean FA across the brain of the youngest PS individual (0.44) is approximately 0.01 (~2.5%) lower than that estimated in TD. Moreover, as there is no age-by-diagnosis interaction, this difference in FA is consistent across ages within our sample. This is clearly demonstrated in Fig. 2a.

While most structural MRI work in individuals along the psychosis spectrum has focused on gray matter disruption, there is compelling evidence that dysfunction of brain WM, specifically in oligodendrocytes and myelin formation, significantly contributes to psychosis (see [64]). Myelination begins postnatally, but completes in young adulthood. Critically, reduced expression of genes associated with components of WM—oligodendrocytes and myelin—are widely replicated in SZ [64] and abnormal oligodendrocyte function is speculated as a primary mechanism in SZ [65].

Thus, it is plausible that altered expression of specific neurotransmitter receptors on oligodendrocytes, which has been shown in demyelinating disorders [66, 67], could be one mechanism of neuronal dysfunction in psychosis. Our results do not suggest that critical changes in brain WM occur during this period—approximately during the same period when the incidence of SZ increases—but they may indicate specific failures of brain cytoarchitecture that predispose individuals to more serious clinical symptoms. Moreover, it is possible that deficits in brain WM, along with other clinical and behavioral symptoms during this time period, would increase confidence in the at-risk diagnosis.

Despite the large-scale nature of the PNC, several limitations should be considered. First, the PNC was set as a cross-sectional study, but particular samples of interest have been followed-up in targeted, yet smaller, investigations. Thus, the current longitudinal study, while one of the largest to date to implement diffusion MRI in youth at risk for developing psychosis, remains relatively small. In addition, we focused our analysis on individuals with persistent psychosis symptoms over two consecutive assessments. There are, however, individuals with inconsistent clinical symptoms that may provide valuable insight. However, these individuals may have more heterogeneity in clinical symptoms and likely brain phenotypes. Unlike some previous imaging studies, we only found *lower* FA and higher diffusivity values in psychosis spectrum youth. Other studies report *elevated* FA in CHR [68] or *no difference* between CHR and healthy individuals [69, 70]. These inconsistencies may stem from relatively small at-risk

samples, heterogeneity of disease course, lack of quality assurance and differences in DTI methodology. While our study is relatively small, the sample is well characterized and followed longitudinally. In addition, we believe our comprehensive approach to data QA and use of a study-specific template are strengths that reduce analytic error. Regions of significantly lower FA in the whole brain analysis did not correspond directly to the regional effects. While the skeletonized approach allows for a whole brain method, TBSS is limited in inferences that can be made at the level of the individual tract. Thus, we included complementary approaches, which incorporated voxelwise and regional approach, to improve specificity of reported deficits. Alterations in the corticospinal tract in at-risk individuals suggests that WM deficits may be linked to motoric disturbances or psychomotor slowing noted in psychosis [71, 72]. What role these motoric disturbances play in the associated cognitive performance deficits remains unknown and should be further investigated. Our follow-up time is restricted to 20 months and longer inter-scan intervals (or additional scans) will likely improve our ability to map meaningful individual change. Yet, importantly, we show that diffusion metrics are, on average, consistent within individuals by estimating the ICCs between diffusion time points. Finally, we find significant associations between AD and MD with cognitive performance, but find no group difference in AD or MD. This finding may suggest dimensional features of brain WM that need to be further explored with respect to symptoms and cognition, as it is unlikely that there are specific cut-points in symptoms or performance that separate those at-risk for psychosis and TD youth.

In conclusion, we measured WM microstructure in a targeted subsample of the PNC, a community sample of youth with and without persistent psychosis spectrum symptoms. We found convergent results demonstrating localized disruptions of WM microstructure in youth with persistent psychotic-like symptoms compared to TD youth. These abnormalities were prominent within the corticospinal tracts and the CB of the hippocampus. These results suggest that youth with persistent psychotic-risk symptoms have similar patterns of WM microstructure abnormalities to those seen in clinically ascertained at-risk samples. It does not appear that these deficits depend on duration of subthreshold symptoms or the confounding influence of psychotropic medication, as very few of these individuals were receiving medication and exclusion of medicated individuals does not change the pattern of results. Taken together we believe that WM microstructure is a meaningful brain phenotype that should be measured and monitored throughout early development. Reliable identification of a "true" psychosis prodrome that signals the onset of a psychotic illness, especially early in its course, is a significant

challenge. The presence of robust abnormalities, such as alterations in brain WM, would increase confidence in the at-risk "diagnosis", while an entirely normal profile might help to identify false positives and thus alleviate some clinical concerns.

Compliance with ethical standards

References

1. Rapoport JL, Giedd JN, Gogtay N. Neurodevelopmental model of schizophrenia: update 2012. Mol Psychiatry. 2012;17:1228–38.
2. Zeidler J, Slawik L, Fleischmann J, Greiner W. The costs of schizophrenia and predictors of hospitalisation from the statutory health insurance perspective. Health Econ Rev. 2012;2:1–8.
3. Gur RE, Turetsky BI, Cowell PE, Finkelman C, Maany V, Grossman RI, et al. Temporolimbic volume reductions in schizophrenia. Arch Gen Psychiatry. 2000;57:769–75.
4. Selemon LD, Goldman-Rakic PS. The reduced neuropil hypothesis: a circuit based model of schizophrenia. Biol Psychiatry. 1999;45:17–25.
5. Laruelle M, Kegeles LS, Abi-Dargham A. Glutamate, dopamine, and schizophrenia. Ann N Y Acad Sci. 2006;1003:138–58.
6. Marsman A, van den Heuvel MP, Klomp DWJ, Kahn RS, Luijten PR, Pol HEH. Glutamate in schizophrenia: a focused review and meta-analysis of 1H-MRS studies. Schizophr Bull. 2011;39:120–9.
7. Kyriakopoulos M, Bargiotas T, Barker GJ, Frangou S. Diffusion tensor imaging in schizophrenia. Eur Psychiatry. 2008;23:255–73.
8. Roalf DR, Ruparel K, Verma R, Elliott MA, Gur RE, Gur RC. White matter organization and neurocognitive performance variability in schizophrenia. Schizophr Res. 2013;143:172–8.
9. McGlashan TH, Hoffman RE. Schizophrenia as a disorder of developmentally reduced synaptic connectivity. Arch Gen Psychiatry. 2000;57:637–48.
10. Pettersson-Yeo W, Benetti S, Marquand A, Dell,ÄòAcqua F, Williams S, Allen P, et al. Using genetic, cognitive and multi-

modal neuroimaging data to identify ultra-high-risk and first-episode psychosis at the individual level. Psychol Med. 2013;43:1–16.

11. Barbato M, Colijn MA, Keefe RS, Perkins DO, Woods SW, Hawkins KA, et al. The course of cognitive functioning over six months in individuals at clinical high risk for psychosis. Psychiatry Res. 2012;206:195–9.

12. Cannon TD, Cadenhead K, Cornblatt B, Woods SW, Addington J, Walker E, et al. Prediction of psychosis in youth at high clinical risk: a multisite longitudinal study in North America. Arch Gen Psychiatry. 2008;65:28–37.

13. Calkins ME, Moore TM, Merikangas KR, Burstein M, Satterthwaite TD, Bilker WB, et al. The psychosis spectrum in a young US community sample: findings from the Philadelphia Neurodevelopmental Cohort. World Psychiatry. 2014;13:296–305.

14. Calkins ME, Merikangas KR, Moore TM, Burstein M, Behr MA, Satterthwaite TD, et al. The Philadelphia Neurodevelopmental Cohort: constructing a deep phenotyping collaborative. J Child Psychol Psychiatry. 2015;56:1356–69.

15. Fusar-Poli P, Bonoldi I, Yung AR, Borgwardt S, Kempton MJ, Valmaggia L, et al. Predicting psychosis: meta-analysis of transition outcomes in individuals at high clinical risk. Arch Gen Psychiatry. 2012;69:220.

16. Roalf D, Nanga R, Rupert P, Hariharan H, Quarmley M, Calkins M, et al. Glutamate imaging (GluCEST) reveals lower brain GluCEST contrast in patients on the psychosis spectrum. Mol Psychiatry. 2017;22:1298–305.

17. Chan RC, Di X, McAlonan GM, Gong Q-y. Brain anatomical abnormalities in high-risk individuals, first-episode, and chronic schizophrenia: an activation likelihood estimation meta-analysis of illness progression. Schizophr Bull. 2011;37:177–88.

18. Karlsgodt KH, Niendam TA, Bearden CE, Cannon TD. White matter integrity and prediction of social and role functioning in subjects at ultra-high risk for psychosis. Biol Psychiatry. 2009;66:562–9.

19. Basser PJ, Mattiello J, LeBihan D. MR diffusion tensor spectroscopy and imaging. Biophys J. 1994;66:259.

20. Le Bihan D, Mangin JF, Poupon C, Clark CA, Pappata S, Molko N, et al. Diffusion tensor imaging: concepts and applications. J Magn Reson Imaging. 2001;13:534–46.

21. Epstein KA, Cullen K, Mueller B, Lee S, Kumre S. White matter abnormalities and cognitive impairment in early-onset schizophrenia-spectrum disorders. J Am Acad Child Adolesc Psychiatry. 2013;53:362–72.

22. White T, Kendi ATK, Lehéricy S, Kendi M, Karatekin C, Guimaraes A, et al. Disruption of hippocampal connectivity in children and adolescents with schizophrenia—a voxel-based diffusion tensor imaging study. Schizophr Res. 2007;90:302–7.

23. Kelly S, Agartz N, Andreassen OA, Fatourous-Bergman H, Brouwer R, Cahn W, et al. White matter differences in schizophrenia: meta-analytic findings from ENIGMA-schizophrenia DTI. Mol Psychiatry. 2018;23:1261–9.

24. Cooper S, Alm KH, Olson IR, Ellman LM. White matter alterations in individuals experiencing attenuated positive psychotic symptoms. Early Interv Psychiatry. 2018;12:372–9.

25. Krakauer K, Ebdrup B, Glenthøj B, Raghava J, Nordholm D, Randers L, et al. Patterns of white matter microstructure in individuals at ultra-high-risk for psychosis: associations to level of functioning and clinical symptoms. Psychol Med. 2017;47:2689–707.

26. Samartzis L, Dima D, Fusar-Poli P, Kyriakopoulos M. White matter alterations in early stages of schizophrenia: a systematic review of diffusion tensor imaging studies. J Neuroimaging. 2014;24:101–10.

27. Tamnes CK, Agartz I. White matter microstructure in early-onset schizophrenia: a systematic review of diffusion tensor imaging studies. J Am Acad Child Adolesc Psychiatry. 2016;55:269–79.

28. Douaud G, Mackay C, Andersson J, James S, Quested D, Ray MK, et al. Schizophrenia delays and alters maturation of the brain in adolescence. Brain. 2009;132:2437–48.

29. Epstein KA, Kumra S. White matter fractional anisotropy over two time points in early onset schizophrenia and adolescent cannabis use disorder: a naturalistic diffusion tensor imaging study. Psychiatry Res. 2015;232:34–41.

30. Saito J, Hori M, Nemoto T, Katagiri N, Shimoji K, Ito S, et al. Longitudinal study examining abnormal white matter integrity using a tract-specific analysis in individuals with a high risk for psychosis. Psychiatry Clin Neurosci. 2017;71:530–41.

31. Krakauer K, Nordentoft M, Glenthøj B, Raghava J, Nordholm D, Randers L, et al. White matter maturation during 12 months in individuals at ultra-high-risk for psychosis. Acta Psychiatr Scand. 2018;137:65–78.

32. Satterthwaite TD, Elliott MA, Ruparel K, Loughead J, Prabhakaran K, Calkins ME, et al. Neuroimaging of the Philadelphia neurodevelopmental cohort. Neuroimage. 2014;86:544–53.

33. Gur RC, Calkins ME, Satterthwaite TD, Ruparel K, Bilker WB, Moore TM, et al. Neurocognitive growth charting in psychosis spectrum youths. JAMA Psychiatry. 2014;71:366–74.

34. Satterthwaite TD, Connolly JJ, Ruparel K, Calkins ME, Jackson C, Elliott MA, et al. The Philadelphia Neurodevelopmental Cohort: a publicly available resource for the study of normal and abnormal brain development in youth. Neuroimage. 2016;124:1115–9.

35. Moore T, Martin I, Gur O, Jackson C, Scott J, Calkins M, et al. Characterizing social environment's association with neurocognition using census and crime data linked to the Philadelphia Neurodevelopmental Cohort. Psychol Med. 2016;46:599–610.

36. Calkins ME, Moore TM, Satterthwaite TD, Wolf DH, Turetsky BI, Roalf DR, et al. Persistence of psychosis spectrum symptoms in the Philadelphia Neurodevelopmental Cohort: a prospective two-year follow-up. World Psychiatry. 2017;16:62–76.

37. Turetsky BI, Moberg PJ, Quarmley M, Dress E, Calkins ME, Ruparel K, et al. Structural anomalies of the peripheral olfactory system in psychosis high-risk subjects. Schizophr Res. 2018;195:197–205.

38. Miller TJ, McGlashan TH, Woods SW, Stein K, Driesen N, Corcoran CM, et al. Symptom assessment in schizophrenic prodromal states. Psychiatr Q. 1999;70:273–87.

39. Endicott J, Spitzer RL, Fleiss JL, Cohen J. The global assessment scale. A procedure for measuring overall severity of psychiatric disturbance. Arch Gen Psychiatry. 1976;33:766–71.

40. Moore TM, Reise SP, Gur RE, Hakonarson H, Gur RC. Psychometric properties of the Penn Computerized Neurocognitive Battery. Neuropsychology. 2015;29:235.

41. Roalf DR, Quarmley M, Elliott MA, Satterthwaite TD, Vandekar SN, Ruparel K, et al. The impact of quality assurance assessment on diffusion tensor imaging outcomes in a large-scale population-based cohort. Neuroimage. 2016;125:903–19.

42. Smith SM. Fast robust automated brain extraction. Hum Brain Mapp. 2002;17:143–55.

43. Andersson JL, Sotiropoulos SN. An integrated approach to correction for off-resonance effects and subject movement in diffusion MR imaging. Neuroimage. 2016;125:1063–78.

44. Graham MS, Drobnjak I, Zhang H. Realistic simulation of artefacts in diffusion MRI for validating post-processing correction techniques. Neuroimage. 2016;125:1079–94.

45. Zhang H, Yushkevich PA, Alexander DC, Gee JC. Deformable registration of diffusion tensor MR images with explicit orientation optimization. Med Image Anal. 2006;10:764–85.

46. Giedd JN, Blumenthal J, Jeffries NO, Castellanos FX, Liu H, Zijdenbos A, et al. Brain development during childhood and adolescence: a longitudinal MRI study. Nat Neurosci. 1999;2:861–3.

47. Peters BD, Ikuta T, DeRosse P, John M, Burdick KE, Gruner P, et al. Age-related differences in white matter tract microstructure are associated with cognitive performance from childhood to adulthood. Biol Psychiatry. 2014;75:248–56.

48. Wood SN Stable and efficient multiple smoothing parameter estimation for generalized additive models. J Am Stat Assoc. 2004;99:673–86.

49. Wood SN. Fast stable restricted maximum likelihood and marginal likelihood estimation of semiparametric generalized linear models. J R Stat Soc. 2011;73:3–36.

50. Satterthwaite TD, Wolf DH, Calkins ME, Vandekar SN, Erus G, Ruparel K, et al. Structural brain abnormalities in youth with psychosis spectrum symptoms. JAMA Psychiatry. 2016;73:515–24.

51. Satterthwaite TD, Shinohara RT, Wolf DH, Hopson RD, Elliott MA, Vandekar SN, et al. Impact of puberty on the evolution of cerebral perfusion during adolescence. Proc Natl Acad Sci. 2014;111:8643–8.

52. Garcia de la Garza A, Vandekar S, Roalf DR, Ruparel K, Gur RC, Gur RE, et al. voxel: Mass-Univarite Voxelwise Analysis of Medical ImagingData. R package version132. 2017. https://rdrr.io/cran/voxel/

53. Winkler AM, Ridgway GR, Webster MA, Smith SM, Nichols TE. Permutation inference for the general linear model. Neuroimage. 2014;92:381–97.

54. Bach M, Laun FB, Leemans A, Tax CM, Biessels GJ, Stieltjes B, et al. Methodological considerations on tract-based spatial statistics (TBSS). Neuroimage. 2014;100:358–69.

55. Shou H, Eloyan A, Lee S, Zipunnikov V, Crainiceanu A, Nebel M, et al. Quantifying the reliability of image replication studies: the image intraclass correlation coefficient (I2C2). Cogn Affect Behav Neurosci. 2013;13:714–24.

56. R-Core-Team. R: A Language and Enviroment for Statistical Computing. Vienna, Austria: R Foundation for Statistical Computing; 2012.

57. Roalf DR, Gur RE, Verma R, Parker WA, Quarmley M, Ruparel K, et al. White matter microstructure in schizophrenia: associations to neurocognition and clinical symptomatology. Schizophr Res. 2015;161:42–49.

58. Beevor CE. On the course of the fibres of the cingulum and the posterior parts of the corpus callosum and fornix in the marmoset monkey. Philos Trans R Soc Lond B. 1891;182:135–99.

59. Brodal A. Neurological anatomy in relation to clinical medicine. USA: Oxford University Press; 1981.

60. Schmahmann JD, Pandya DN, Wang R, Dai G, D'arceuil HE, de Crespigny AJ, et al. Association fibre pathways of the brain: parallel observations from diffusion spectrum imaging and autoradiography. Brain. 2007;130:630–53.

61. Goldman-Rakic PS, Selemon LD, Schwartz ML. Dual pathways connecting the dorsolateral prefrontal cortex with the hippocampal formation and parahippocampal cortex in the rhesus monkey. Neuroscience. 1984;12:719–43.

62. Jones DK, Knösche TR, Turner R. White matter integrity, fiber count, and other fallacies: the do's and don'ts of diffusion MRI. Neuroimage. 2013;73:239–54.

63. Buckner RL. Memory and executive function in aging and AD: multiple factors that cause decline and reserve factors that compensate. Neuron. 2004;44:195–208.

64. Takahashi N, Sakurai T, Davis KL, Buxbaum JD. Linking oligodendrocyte and myelin dysfunction to neurocircuitry abnormalities in schizophrenia. Prog Neurobiol. 2011;93:13–24.

65. Mighdoll MI, Tao R, Kleinman JE, Hyde TM. Myelin, myelin-related disorders, and psychosis. Schizophr Res. 2015;161:85–93.

66. Newcombe J, Uddin A, Dove R, Patel B, Turski L, Nishizawa Y, et al. Glutamate receptor expression in multiple sclerosis lesions. Brain Pathol. 2008;18:52–61.

67. Werner P, Pitt D, Raine CS. Multiple sclerosis: altered glutamate homeostasis in lesions correlates with oligodendrocyte and axonal damage. Ann Neurol. 2001;50:169–80.

68. Schmidt A, Lenz C, Smieskova R, Harrisberger F, Walter A, Riecher-Rössler A, et al. Brain diffusion changes in emerging psychosis and the impact of state-dependent psychopathology. Neurosignals. 2015;23:71–83.

69. Thomas C, Moya L, Avidan G, Humphreys K, Jung KJ, Peterson MA, et al. Reduction in white matter connectivity, revealed by diffusion tensor imaging, may account for age-related changes in face perception. J Cogn Neurosci. 2008;20:268–84.

70. Peters BD, Blaas J, de Haan L. Diffusion tensor imaging in the early phase of schizophrenia: what have we learned? J Psychiatr Res. 2010;44:993–1004.

71. De Weijer A, Mandl R, Diederen K, Neggers S, Kahn R, Pol HH, et al. Microstructural alterations of the arcuate fasciculus in schizophrenia patients with frequent auditory verbal hallucinations. Schizophr Res. 2011;130:68–77.

72. Ublinskii M, Semenova N, Lukovkina O, Sidorin S, Lebedeva I, Kaleda V, et al. Characteristics of diffusion in the corticospinal tract of patients with early stage of schizophrenia: diffusion tensor magnetic resonance imaging. Bull Exp Biol Med. 2015;159:29.